

Luminescent Sensing and Catalytic Performances of a Multifunctional Lanthanide-Organic Framework Comprising a Triphenylamine Moiety

Pengyan Wu, Jian Wang, Yaming Li,* Cheng He, Zhong Xie, and Chunying Duan*

A multifunctional lanthanide-organic framework Tb–TCA ($H_3TCA =$ tricarboxytriphenylamine) comprising a triphenylamine moiety as an efficient luminescence sensitizer is synthesized by a solvothermal method and structurally characterized. Tb–TCA exhibits lanthanide-based emission (540 nm) and triphenylamine emission (435 nm) after excitation at 350 nm and works as a luminescent chemosensor towards salicylaldehyde with a sensitivity of 10 ppm under optimized conditions. Tb–TCA features a high concentration of Lewis acid Tb^{3+} sites and Lewis base triphenylamine sites on its internal surfaces; it thus enables both Knoevenagel and cyanosilylation reactions in a size-selective fashion. The ratiometric fluorescent response towards aldehydes (I_{540}/I_{435}) demonstrates that the absorption of the porous material is size selective, and the interactions between the aldehyde molecules and the Tb^{3+} ions play a dominant role in the absorption and activation of the aldehyde substrates. In particular, these studies provide opportunities to directly validate the sorption sites and the catalytic mechanism of the multifunctional Ln metal–organic framework material by luminescence.

1. Introduction

Among the porous polycarboxylate-based metal–organic frameworks (MOFs),^[1] the field of lanthanide MOFs (LnMOFs) with two- or three-dimensional structures is rapidly growing, because of the discovery of new crystalline structures that exhibit interesting properties and have potential applications in catalysis, contrast agents, nonlinear optics, photoluminescent, and electroluminescent devices.^[2] One of the extensively investigated approaches is to immobilize unsaturated Lewis acid Ln ions within relatively open frameworks with well-defined pores. This approach enables us to target unique porous LnMOFs with multifunctional properties and catalytic applications.^[3] However, reports on catalytic studies of lanthanide-organic frameworks are relatively scarce compared to the large number of LnMOFs reported,^[4] especially no experimental data regarding the catalytic mechanisms in lanthanide-organic frameworks seems to be available. Such fundamental studies are essential,

however, for the optimization of this new class of lanthanide-organic frameworks for practical catalysis applications.

On the other hand, lanthanide-based porous metal-organic frameworks are excellent candidates to create multifunctional materials for chemosensors, provided their photoluminescence and emission lifetimes are not influenced by solvent molecules at ambient conditions. However, as the forbidden and faint intraconfiguration f–f transitions of lanthanide ions results in absorption coefficients smaller than $10 M^{-1}cm^{-1}$,^[5] targeting porosity and luminescence in a MOF further restricts the choices of building blocks, thus, in addition to being able to sustain porosity the ligand should also act as an antenna to sensitize Ln ions.^[6]

With those parameters in mind, we created a multifunctional lanthanide-organic framework Tb–TCA ($H_3TCA =$ tricarboxytriphenylamine), **Scheme 1**, through incorporating a triphenylamine moiety as an efficient luminescence sensitizer.^[7] We reasoned that the Tb^{3+} ions exposed on the surface of the framework might serve as potential Lewis acids, and the triphenylamine located around the cavity of the MOF would provide a base-like catalyzing force^[8] for special reactions. Tb–TCA was also expected to exhibit bright emission sensitive to the chemical reactants or products encapsulated, with a ratiometric response that could be used to examine the roles of the Lewis acid (Ln^{3+} interactions activate sites) and base (triphenylamine interaction sites) catalytic forces on the substrates incorporated.

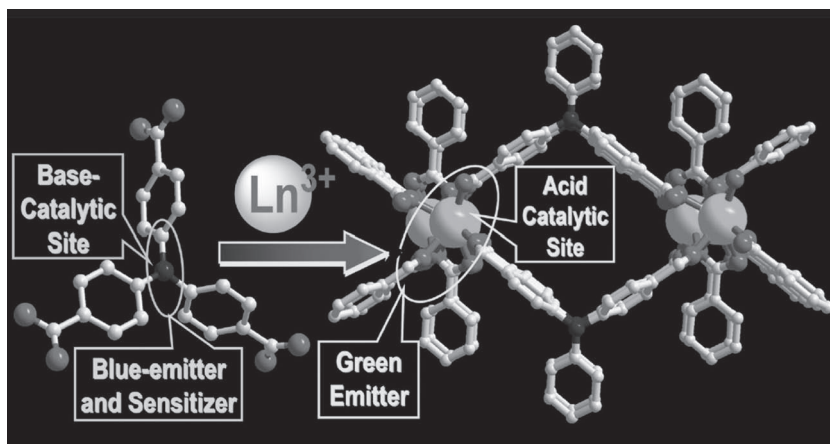
2. Results and Discussions

2.1. Synthesis and Characterization of Tb–TCA

The solvothermal reaction of H_3TCA and $Tb(NO_3)_3 \cdot 6H_2O$ in mixed solvents of dimethylformamide (DMF) and ethanol gave compound Tb–TCA in a high yield (75%). Elemental analyses and powder X-ray analysis indicated the pure phase of its bulky sample. Thermogravimetric analysis (TGA) demonstrated that in the range of 25–200 °C, the TGA curve exhibited an initial weight loss of 10.9%, corresponding to the loss of one dimethyl formamide molecule (expected 10.7%), indicating that the framework of Tb–TCA was stable below

Dr. P. Wu, J. Wang, Y. Li, C. He, Z. Xie, Prof. C. Duan
State Key Laboratory of Fine Chemicals
Dalian University of Technology
Dalian 116012, P. R. China
E-mail: cyduan@dlut.edu.cn; ymli@dlut.edu.cn

DOI: 10.1002/adfm.201100115



Scheme 1. Perspective views of channels within multifunctional MOF Tb-TCA showing the constitutive/constructional fragments

200 °C. This property is one of the essential factors for a good heterogeneous catalyst.

Single-crystal structure analysis reveals the presence of a non-interpenetrating 3D network comprising one-dimensional channels. The coordination environment around Tb^{3+} is shown in **Figure 1**. Each terbium ion is coordinated by four oxygen atoms of four di-monodentate carboxyl groups, two oxygen atoms of a bidentate carboxyl group, one μ_2 -oxygen atom of another bidentate carboxyl group, and one oxygen atom from a DMF molecule. The di-monodentate carboxyl groups act as a four-fold bridge, linking to another Tb^{3+} ion to form a dimeric unit. This dimeric unit connects neighbors through two centrosymmetric μ_2 -oxygen atoms of the didentate carboxyl groups, forming a one-dimensional pillar along the *a* axis. These TCA ligands connected the pillars to form three-dimensional frameworks with channels along the direction defined by the *a* axis. The nitrogen atoms are located around the cavities, providing base catalyzing forces. It should be noted that the immobilization of Lewis-basic sites within porous MOFs, however, has been a challenge, because such Lewis basic sites tend to bind other metal ions to form condensed structures. The cross-section of the running channel is a tetragon consolidated by two centrosymmetric Tb^{3+} ions and two TCA ligands with dimensions of $7.5 \text{ \AA} \times 8.5 \text{ \AA}$, which are available for guest accommodation and exchange. The metal centers with removable solvent molecules are well-positioned in the channels to interact with guest molecules that enter the framework pores, suggesting that Tb-TCA should be also an active heterogeneous catalyst for Lewis acid promoted reactions.^[9]

2.2. Luminescence and Sensing Studies

Solid state UV-vis absorption spectra of Tb-TCA exhibited an intense absorption band centered at 350 nm, that can be assigned to the $\pi-\pi^*$ transition of the triphenylamine group.^[10] Since the triphenylamine emitter is an efficient sensitizer to prompt the corresponding luminescence, characteristic Tb^{3+} emissions, which can be assigned to the transitions of $^5D_4 \rightarrow ^7F_3$, $^5D_4 \rightarrow ^7F_5$, and $^5D_4 \rightarrow ^7F_6$ when excited at 350 nm,^[11] are

observed beside the emission of the triphenylamine group centered about 435 nm. As can be expected, these luminescences were strongly quenched (>99% quench percentage) when salicylaldehyde (SA) was incorporated (**Figure 2**).

To quantitatively investigate the quenching process, fluorescent measurements were carried out in a 1 cm quartz cuvette on a suspension of Tb-TCA. The addition of SA to the suspension of Tb-TCA caused significant luminescence quenching of both emission bands and led to an obvious diminishing of the green emission under UV-light excitation. Under optimized conditions, the detection limit of the MOF (4 ppm in CH_2Cl_2 solution) towards SA is established at or below 10 ppm (ca. 0.2 mM),

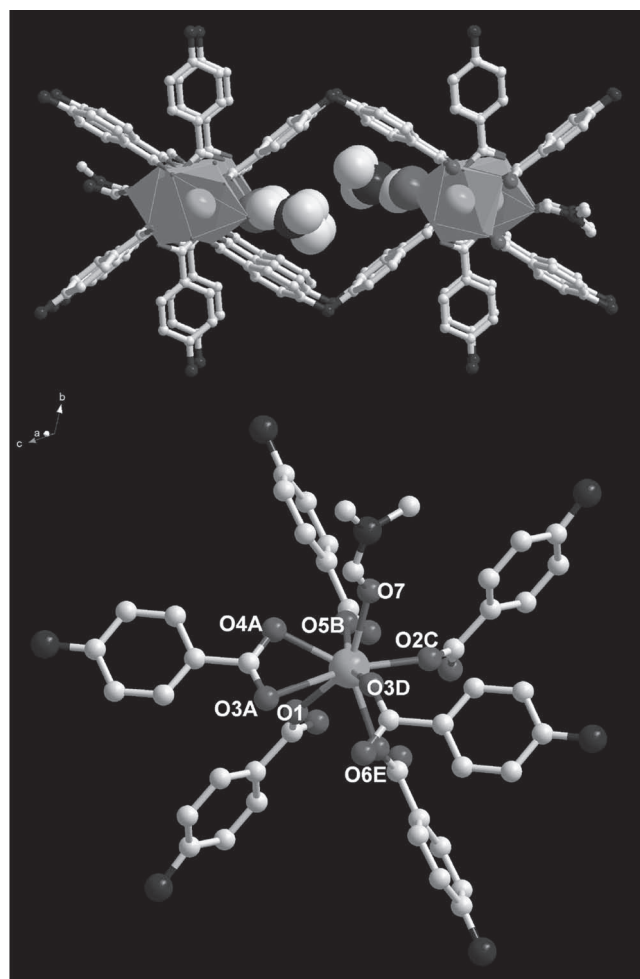


Figure 1. View of the crystal packing of Tb-TCA along the *a* direction showing the rhombic channels, with exposed coordinated unsaturated metal ions and nitrogen atoms, and the coordination configuration of the metal center. Selected bond distances (\AA) are: Tb(1)–O(5B) 2.276(4), Tb(1)–O(2C) 2.303(4), Tb(1)–O(1) 2.323(4), Tb(1)–O(3A) 2.341(4), Tb(1)–O(6E) 2.363(4), Tb(1)–O(4A) 2.378(3), Tb(1)–O(7) 2.427(4), Tb(1)–O(3D) 2.865(4). Symmetry codes: A. $1-x, 1-y, -z+2$; B. $x, 1+y, z$; C. $-x, 1-y, 1-z$; D. $x, y, -1+z$; E. $-x, -y, 1-z$.

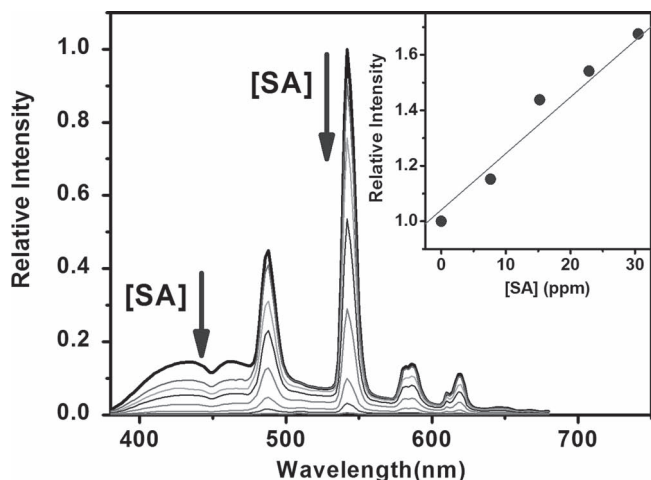


Figure 2. Family of luminescent spectra of Tb–TCA emulsion in CH_2Cl_2 upon addition of various amounts of salicylaldehyde (SA) up to 2 mM. The insert showing emission intensities at 540 nm as a function of SA in the lower concentration range (10 to 30 ppm). Excitation at 350 nm.

and the reduction in luminescence intensity is proportional to the concentration of the aldehyde.

The quenching effect is rationalized by the Stern–Volmer equation:^[12]

$$I_0 I = 1 + K_{SV}[M]$$

The values I_0 and I are the luminescence intensities of aldehyde-free Tb–TCA and aldehyde-incorporated Tb–TCA, respectively, $[M]$ is the molar concentration of the aldehydes added, and K_{SV} is the quenching-effect coefficient of the aldehyde. K_{SV} was calculated from the experimental data for the examined aldehyde. The high quenching effect coefficient (K_{SV}) of ca. 2400 M^{-1} and the low detection limit for SA allowed us to easily identify the existence of a small amount of aldehyde in solution. And since the emission wavelength is hardly varied during the addition of SA, the fluorescence-quenching effect of the aldehydes was ascribed to a photo-induced energy transfer (PET) mechanism from the guest molecules to the excited state of the triphenylamine groups.^[13]

Interestingly, K_{SV} values referring to the intensities at 435 nm (triphenylamine emission) and at 540 nm (the Tb^{3+} emission) are different (Figure 3). With the decrease of the intensities of the two emission bands upon incorporating SA, the I_{540}/I_{435} ratio increases significantly, since the two emission bands were isogenous, and the characteristic Tb^{3+} emission was prompted by the excitation of the triphenylamine group. The quenching of the two emission bands was attributed to PET from the triphenylamine group to SA, whereas the increase of the I_{540}/I_{435} ratio should be attributed to the interactions between SA molecules and Tb^{3+} ions. Accordingly, the enhancement of the emitting efficiency at 540 nm (Tb^{3+} characteristic emission) was attributed to the replacement of the coordinated solvent molecules by aldehydes. The potential of luminescent MOFs for sensing functions was proposed a decade ago; however, this emerging ratiometric chemosensor is very significant, as it can eliminate most or all ambiguities (i.e., canceling artifacts due to variations in probe concentration,

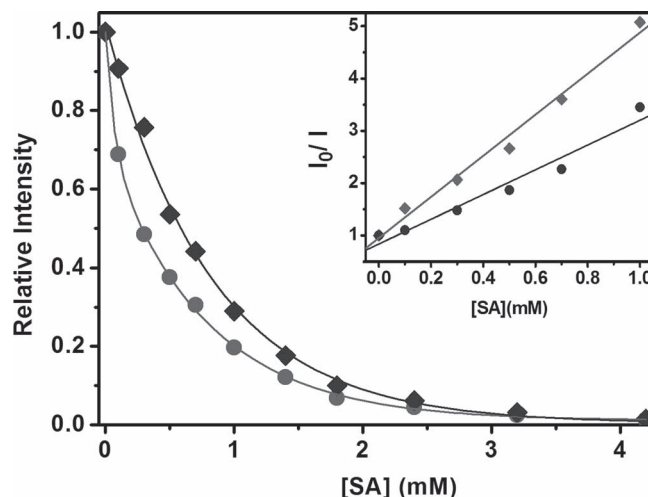


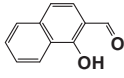
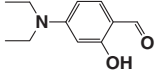
Figure 3. Fluorescence responses of Tb–TCA upon addition of SA in CH_2Cl_2 at 540 nm (square marks) and at 435 nm (dot marks). Excitation at 350 nm. The inset shows the quenching effect coefficients (K_{SV}) of SA at the above-mentioned emission bands, excited at 350 nm. The values I_0 and I represent the luminescence intensities of aldehyde-free Tb–TCA and aldehyde-incorporated Tb–TCA, respectively.

probe environment, and excitation intensity) by self-calibration of two emission bands.^[14]

2.3. Knoevenagel Condensation Reaction Catalyzed by Tb–TCA Materials

Inspired by the very few example of porous MOFs with Lewis-basic sites including amides sites,^[15] the Knoevenagel reaction, which requires the formation of an anion of the active methylene-containing basic compound,^[16] was used to highlight the significance of the functional properties of Tb–TCA. As shown in Table 1, the loading of a molar ratio of only 2%

Table 1. Knoevenagel reaction of salicylaldehyde derivatives with malononitrile catalyzed by Tb–TCA. Reaction conditions: malononitrile: 1.2 mmol, aldehyde: 0.5 mmol, Tb–TCA catalysts: 0.01 mmol (2 mol%); room temperature for 6 h.

$\text{R}-\text{C}_6\text{H}_3(\text{OH})-\text{CHO} + \text{NC}-\text{CH}_2-\text{CN} \xrightarrow[\text{CH}_2\text{Cl}_2]{\text{Tb-TCA}} \text{R}-\text{C}_6\text{H}_3(\text{OH})-\text{C}(\text{CN})=\text{CH}-\text{NH}$	
Substrate	Conversion (%) ^{a)}
	99
	23
	<2

^{a)}Conversion based on aldehydes.

of Tb–TCA lead to over 90% conversion of salicylaldehyde. The catalysis efficiency of Tb–TCA was comparable to the best results obtained previously for MOFs, a yield of 98% obtained after 12 h.^[15] In contrast, the conversion yield for 2-hydroxy-1-naphthaldehyde (NSA), with molecular dimensions of 9.7 Å × 8.4 Å,^[17] is reduced to about 20%, under similar experimental conditions. The presence of 5-(diethylamino)salicylaldehyde (DSA) only causes a trace conversion under the same experimental conditions. One would expect a comparable reactivity, thus this experiment suggests that the 8.5 Å wide section in Tb–TCA is too small to accommodate the transition-state geometry required for activating these substrates, indicating that the activation of the carbonyl species occurs inside the channels, not on the surface of the solid catalyst. Since the Knoevenagel reactions could not take place in the absence of the catalyst Tb–TCA, this set of experiments demonstrates that Tb–TCA is a real catalyst with at least the aromatic aldehydes accessing the catalytic sites via the cavity.

To confirm the selective accommodation and activation of reactants by Tb–TCA, adsorption experiments were performed. Adding Tb–TCA (50 mg) to a dichloromethane solution containing substrates and stirring for 12 h afforded new crystalline solids. These crystalline solids are difficult to dissolve in any solvent, thus deuterium chloride was used to destroy the MOF structure in order to increase their solubility. ¹H NMR spectra (Figure 4) show that Tb–TCA adsorbed 3, 1, and 0.8 equivalents of SA, NSA and DSA per triphenylamine moiety, implying that the smaller molecule was more easily introduced to the channels of Tb–TCA. Infrared spectroscopy of the catalyst impregnated with a CH₂Cl₂ solution of the reaction solution revealed a C=O stretch vibration at 1687 cm⁻¹. The red shift from 1708 cm⁻¹ (free aldehyde) suggested the sorption of SA and the activation

of the substrate in the channels of the MOFs through interactions between the Tb³⁺ ions and the C=O group of the aldehydes. It seems that, beside the base-type triphenylamine catalytic active sites, the interactions between SA and the Tb³⁺ ions also exhibited excellent activities for this kind of Knoevenagel condensation. While a series of MOFs can catalyze the important reactions through isolated acid and/or base catalyzing forces,^[21] the incorporation of both acid- and base-catalyzing forces within one channel is quite rare. The highest yield achieved in the channels demonstrates their significant to directly enhance the catalytic efficiency.

Furthermore, the luminescent responses for these aldehydes are size-selective. As shown in Figure 5, the addition of 2-NSA and DSA reduced the luminescence of the Tb³⁺ (540 nm) and triphenylamine (435 nm) emissions of the suspension of Tb–TCA in CH₂Cl₂, while the ratio (*I*₅₄₀/*I*₄₃₅) of the two emission intensities did not vary significantly, since the two emission bands were isogenous, and the characteristic Tb³⁺ emission was prompted by the excitation of the triphenylamine group. The quenching of the two emission bands whilst maintaining the ratio (*I*₅₄₀/*I*₄₃₅) suggested the absence of obvious interactions between NSA or DSA and the lanthanide ions. In accord, structural simulations of the substrates demonstrated that the rhombic channels were not large enough to encapsulate molecules of NSA or DSA.

These results all supported that only molecules with suitable sizes have the potential to enter the channels and to interact with the Ln sites, which thus exhibited a size-selective luminescent response. The Lewis-acid Ln sites played a dormant role in the Knoevenagel condensation reactions. Although only a few lanthanide–organic frameworks could be used as efficient catalysts to prompt special interactions,^[4] the validation of the catalytic mechanism of the reactions via ratiometric luminescent responses is very significant. The new approach can be extended to other reactions prompted by Lewis-acid- and/or base-catalyzed forces for sensing and absorbing organic molecules in environmental or organic-synthetic applications.

2.4. Cyanosilylation Reaction Catalyzed by Tb–TCA Materials

Since the addition of cyanide to a carbonyl compound to form a cyanohydrin is one of the fundamental carbon–carbon bond-forming reactions in organic chemistry and has frequently been at the forefront of advances in chemical transformations,^[18] a cyanosilylation reaction was performed with a 1:2.4 molar ratio of the selected 2-nitrobenzaldehyde (2-NBA), 3-nitrobenzaldehyde (3-NBA), 4-nitrobenzaldehyde (4-NBA), 1-naphthylaldehyde(1-NTA), and cyanotrimethylsilane in CH₂Cl₂ at room temperature through a heterogeneous manner. As shown in Table 2, the presence of 2 mol% solid Tb–TCA led to over 75% conversion 2-NBA,

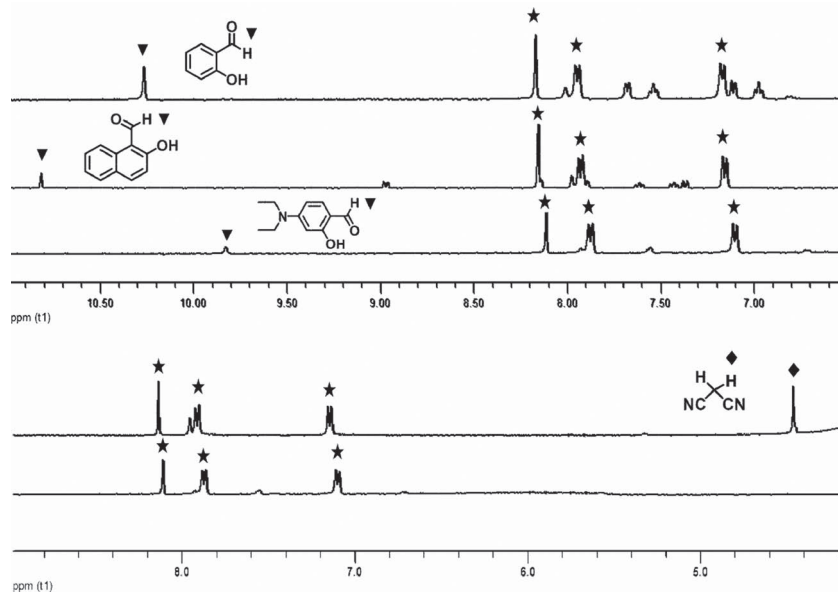


Figure 4. a) ¹H NMR spectra of the powder Tb–TCA that decomposed in DCl:DMSO-*d*₆. b–e) ¹H NMR spectra of the powder Tb–TCA with guest molecules adsorbed that decomposed in DCl:DMSO-*d*₆: malononitrile (b), 5-(diethylamino)salicylaldehyde (DSA) (c), 2-hydroxy-1-naphthaldehyde (NSA) (d), and salicylaldehyde (SA) (e), respectively. The peaks marked with asterisks represent the signals of protonated TCA.

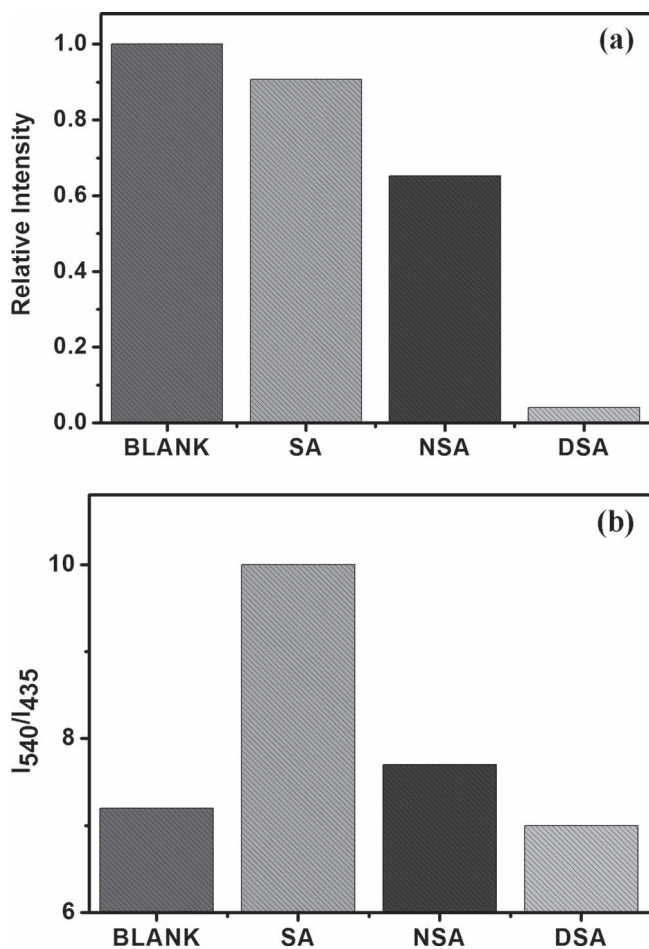
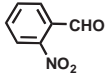
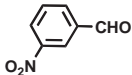
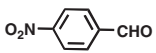


Figure 5. a) Luminescence responses of Tb-TCA to the addition of aldehyde (0.1 mM). Intensities were recorded at 540 nm, excitation at 350 nm. b) The I_{540}/I_{435} ratio of Tb-TCA-CH₂Cl₂ emulsion, blank and after sorption of different SAs (0.1 mM). Excitation at 350 nm.

monitored by ¹H NMR. The catalysing efficiency of Tb-TCA was comparable to the best results previously obtained for MOFs,^[19] a yield of 98% obtained after 16 h, and represents a significant improvement compared to lanthanide bisphosphonates MOFs with a yield lower 70% after 16 h.^[20] Most notably, the use of 2-NBA, a potentially bidentate substrate, resulted in a higher catalytic efficiency. As shown in Table 2, our experiments show a 20% increase in the yield of 2-NBA compared to that of 3-NBA under the same experimental conditions.

It is important to note that the sorption of 2-NBA caused the luminescence quenching of the two bands, and at the same time led to a two-fold increase in the ratio (I_{540}/I_{435}) in comparison to free Tb-TCA, while in the presence of 4-NBA and 3-NBA the change in the ratio (I_{540}/I_{435}) was only minor (Figure 6). The interactions between 2-NBA and Tb-TCA might be similar to that of SA, for which the guest molecules acted as bidentate chelators to coordinate Tb³⁺. Molecules of 3-NBA are unlikely to react as bidentate chelators and thus cannot replace the coordinating solvent molecules on Tb³⁺ as easily. These results demonstrated that the interactions at the Tb³⁺ sites were dominant for ratiometrical luminescent responses and for activating the aldehydes. In this case, the

Table 2. Catalytic cyanosilylation of carbonyl substrates in the presence of Tb-TCA. Reaction conditions: (CH₃)₃SiCN: 1.2 mmol, aldehyde: 0.5 mmol, Tb-TCA catalysts: 0.01 mmol (2 mol%), room temperature under N₂ for 4 h.

$\text{Ar}-\text{CHO} + (\text{CH}_3)_3\text{SiCN} \xrightarrow[\text{CH}_2\text{Cl}_2]{\text{Tb-TCA}} \text{Ar}-\text{CH}(\text{OSi}(\text{CH}_3)_3)\text{CN}$	
Substrate	Conversion (%) ^{a)}
	78
	59
	47
	11

^{a)}Conversion based on aldehydes.

luminescence behavior of Tb-TCA enabled us to validate the sorption properties of the MOFs and, at the same time, to distinguish between possible mechanism of these catalytic reactions.

3. Conclusions

In summary, we reported a new approach to create a multifunctional lanthanide-organic framework Tb-TCA that features a high concentration of Lewis-acidic Tb³⁺ sites and Lewis-basic triphenylamine sites on its internal surfaces. Tb-TCA can catalyze both the Knoevenagel reaction and cyanosilylation in a size-selective fashion through base-type and acid-type catalysis sites, respectively. Further, it exhibits bright lanthanide-based emission simultaneously with the direct emission of triphenylamine. The new approach will be extended to other lanthanide-based MOFs with other luminescent-active lanthanide ions and a series of amino-containing organic dyes to assemble more efficient acid- and/or base-type MOF-based catalysts and luminescent materials for sensing or absorbing organic molecules towards environmental and organic-synthetic applications.

4. Experimental Section

Material and Methods: All chemicals were of reagent-grade quality obtained from commercial sources and used without further purification. ¹H NMR spectra were recorded on a Varian INOVA 400M spectrometer. Powder XRD was performed on a Rigaku D/Max-2400 X-ray diffractometer with a Cu sealed tube ($\lambda = 1.54178 \text{ \AA}$). Elemental analyses were obtained with an Elemental Analyzer Vario EL ? instrument. Thermogravimetric

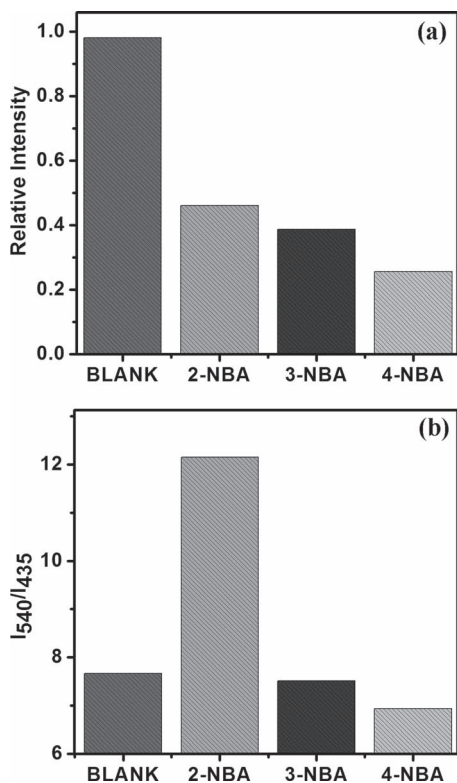


Figure 6. a) Luminescent responses of Tb-TCA upon addition of aldehydes (2 mM). Intensities were recorded at 540 nm, excitation at 350 nm. b) The I_{540}/I_{435} ratio of the Tb-TCA CH_2Cl_2 emulsion, blank and after sorption of different NBAs (2 mM). Excitation at 350 nm.

analysis (TGA) was carried out at a ramp rate of $5\text{ }^\circ\text{C min}^{-1}$ in a nitrogen flow with a Mettler-Toledo TGA/SDTA851 instrument. Fourier-transform infrared (FT-IR) spectra were recorded as KBr pellets on a JASCO FT/IR-430 instrument. Fluorescence spectra of the solution were obtained using the FS920 spectrometer (Edinburgh Instruments). Both excitation and emission slit were 3 nm wide. Fluorescence measurements were carried out in a 1 cm quartz cuvette on a suspension of Tb-TCA excited at 350 nm. The solid fluorescent spectra were measured on JASCO FP-6500.

Synthesis and Crystal Growth: Tb-TCA: A mixture of 4,4',4''-tricarboxytriphenylamine^[21] (H_3TCA) (94 mg, 0.25 mmol) and $\text{Tb}(\text{NO}_3)_3 \cdot 6\text{H}_2\text{O}$ (453 mg, 1 mmol) were dissolved in 15 mL mixed solvents of dimethyl formamide (DMF) and ethanol in a screw-capped vial. The resulting mixture was kept in an oven at $100\text{ }^\circ\text{C}$ for 3 days. Yellow block-shaped crystals were obtained after filtration. Yield: 75%. Anal. calcd. for $\text{C}_{27}\text{H}_{26}\text{N}_3\text{O}_8\text{Tb}$ (%): C, 47.73; H, 3.86; N, 6.18; Found: C, 47.77; H 3.80, N 6.08.

Crystallography of Tb-TCA: $\text{C}_{27}\text{H}_{26}\text{N}_3\text{O}_8\text{Tb}$, $M = 679.43$, triclinic, space group P-1, $a = 8.257(6)\text{ \AA}$, $b = 13.163(10)\text{ \AA}$, $c = 14.238(11)\text{ \AA}$, $\alpha = 114.261(8)$, $\beta = 96.493(9)$, $\gamma = 101.699(9)$, $V = 1347.6(17)\text{ \AA}^3$, $Z = 2$, $D_c = 1.674\text{ g cm}^{-3}$, $\mu(\text{Mo-K}\alpha) = 2.68\text{ mm}^{-1}$, $T = 293(2)\text{ K}$. 4583 unique reflections [$R_{\text{int}} = 0.0676$]. Final R_1 [with $I > 2\sigma(I)$] = 0.0446, wR_2 (all data) = 0.0741, GOOF = 1.028. CCDC 807487 contains the supplementary crystallographic data for this paper. These data can be obtained free of charge from The Cambridge Crystallographic Data Centre via www.ccdc.cam.ac.uk/data_request/cif. Intensities were collected on a Bruker SMART APEX CCD diffractometer with graphite monochromated Mo-K α ($\lambda = 0.71073\text{ \AA}$) using the SMART and SAINT programs. The structure was solved by direct methods and refined on F^2 by full-matrix least-squares methods with SHELXTL version 5.1. Non-hydrogen atoms of the

ligand backbones were refined anisotropically. Hydrogen atoms within the ligand backbones were fixed geometrically at calculated positions and allowed to ride on the parent non-hydrogen atoms. Hydrogen atoms of the carboxylate moieties were found from the difference Fourier maps and refined with the isotropic parameters fixed as 1.5 times of those oxygen atoms they were attached to and with a fixed O-H distance fixed of 0.85 \AA .

Typical Procedure for Knoevenagel Reactions Using the Catalyst Tb-TCA: To a mixture of malononitrile (1.2 mmol) and aromatic aldehyde (0.5 mmol), Tb-TCA (2 mol%) was added. The resulting mixture was stirred at room temperature for 6 h. The reaction was monitored by thin-layer chromatography (TLC). Conversion was determined by ^1H NMR analysis.

Typical Procedure for Asymmetric Cyanosilylation of Aldehydes Using the Catalyst Tb-TCA: To a mixture of TMSCN (1.2 mmol) and aromatic aldehyde (0.5 mmol), Tb-TCA (2 mol%) was added. The resulting mixture was stirred at room temperature for 4 h. The reaction was monitored by TLC. Conversions were determined by ^1H NMR analysis.

Acknowledgements

We gratefully acknowledge financial support from the NNSF (Number: 21025102).

Received: January 17, 2011

Revised: February 15, 2011

Published online: May 31, 2011

- a) S. Kitagawa, R. Kitaura, S. Noro, *Angew. Chem. Int. Ed.* **2004**, *43*, 2334; b) C. N. R. Rao, S. Natarajan, R. Vaidhyanathan, *Angew. Chem. Int. Ed.* **2004**, *43*, 1466; c) R. J. Kupplera, D. J. Timmons, Q.-R. Fanga, J.-R. Li, T. A. Makala, M. D. Younga, D. Yuana, D. Zhao, W. Zhuang, H.-C. Zhou, *Coord. Chem. Rev.* **2009**, *253*, 3042; d) S. L. Qiu, G. S. Zhu, *Coord. Chem. Rev.* **2009**, *253*, 2891; e) J. J. Perry, IV, J. A. Perman, M. J. Zaworotko, *Chem. Soc. Rev.* **2009**, *38*, 1400; f) M. O'Keeffe, *Chem. Soc. Rev.* **2009**, *38*, 1215.
- a) O. Guillou, C. Daiguebonne, in *Handbook on the Physics and Chemistry of Rare Earths*, Vol. 34 (Eds: K. A. Gschneidner, J.-C. G. Bünzli, V. K. Pecharsky), Elsevier, New York **2005**, p. 359; b) J. Rocha, L. D. Carlos, F. A. Almeida Paza, D. Ananias, *Chem. Soc. Rev.* **2011**, *40*, 926; c) R. Sessoli, A. K. Powell, *Coord. Chem. Rev.* **2009**, *253*, 2328; d) D. Farrusseng, S. Aguado, C. Pinel, *Angew. Chem. Int. Ed.* **2009**, *48*, 7502; e) J. Y. Lee, O. K. Farha, J. Roberts, K. A. Scheidt, S. T. Nguyen, J. T. Hupp, *Chem. Soc. Rev.* **2009**, *38*, 1450; f) A. M. Spokoyny, D. Kim, A. Sumrein, C. A. Mirkin, *Chem. Soc. Rev.* **2009**, *38*, 1218; g) C. Janiak, *Dalton Trans.* **2003**, 2781; h) M. D. Allendorf, C. A. Bauer, R. K. Bhaktaa, R. J. T. Houka, *Chem. Soc. Rev.* **2009**, *38*, 1330; i) B. Chen, Y. Yang, F. Zapata, G. Lin, G. Qian, E. B. Lobkovsky *Adv. Mater.* **2007**, *19*, 1693; j) B. Chen, S. Xiang, G. Qian, *Acc. Chem. Res.* **2010**, *43*, 1115.
- a) X. D. Guo, G. S. Zhu, Z. Y. Li, F. X. Sun, Z. H. Yang, S. L. Qiu, *Chem. Commun.* **2006**, 3172; b) F. Gandara, A. de Andres, B. Gomez-Lor, E. Gutierrez-Puebla, M. Iglesias, M. A. Monge, D. M. Prosperio, N. Snejko, *Cryst. Growth Des.* **2008**, *8*, 378; c) M. J. Vitorino, T. Devic, M. Tromp, G. Ferey, M. Visseaux, *Macromol. Chem. Phys.* **2009**, *210*, 1923.
- a) M. Zimmermann, K. W. Tornroos, R. Anwander, *Angew. Chem. Int. Ed.* **2008**, *47*, 775; b) L. Cunha-Silva, S. Lima, D. Ananias, P. Silva, L. Mafra, L. D. Carlos, M. Pillinger, A. A. Valente, F. A. Almeida Paz, J. Rocha, *J. Mater. Chem.* **2009**, *19*, 2618; c) J. Perles, N. Snejko, M. Iglesiasb, M. A. Monge, *J. Mater. Chem.* **2009**, *19*, 6504.
- W. T. Carnall, in *Handbook on the Physics and Chemistry of Rare Earths*, Vol. 3 (Eds: K. A. Gschneidner, L. Eyring), North-Holland, Amsterdam, The Netherlands, **1979**, Ch. 24.

- [6] a) J.-C. G. Bünzli, *Acc. Chem. Res.* **2006**, *39*, 53; b) S. V. Eliseeva, J.-C. G. Bünzli, *Chem. Soc. Rev.* **2010**, *39*, 189.
- [7] a) Y. B. Song, C. Di, X. Yang, S. Li, W. Xu, Y. Liu, L. Yang, Z. Shuai, D. Zhang, D. Zhu, *J. Am. Chem. Soc.* **2006**, *128*, 15940; b) Y. Shang, Y. Wen, S. Li, S. Du, X. He, L. Cai, Y. Li, L. Yang, H. Gao, Y. Song, *J. Am. Chem. Soc.* **2007**, *129*, 11674; c) J. R. Pinzon, D. C. Gasca, S. G. Sankaranarayanan, G. Bottari, T. Torres, D. M. Guldi, L. Echegoyen, *J. Am. Chem. Soc.* **2009**, *131*, 7727.
- [8] a) J. Gascon, U. Aktay, M. D. Hernandez-Alonso, G. P. M. van Klink, F. Kapteijn, *J. Catal.* **2009**, *261*, 75; b) Q. R. Fang, D. Q. Yuan, J. Sculley, J. R. Li, Z. B. Han, H. C. Zhou, *Inorg. Chem.* **2010**, *49*, 11637; c) Y. K. Hwang, D. Y. Hong, J. S. Chang, S. H. Jhung, Y. K. Seo, J. Kim, A. Vimont, M. Daturi, C. Serre, G. Ferey, *Angew. Chem. Int. Ed.* **2008**, *47*, 4144.
- [9] a) M. Fujita, Y. J., Kwon, S. Washizu, K. Ogura, *J. Am. Chem. Soc.* **1994**, *116*, 1151; b) O. Ohnori, M. Fujita, *Chem. Commun.* **2004**, 1586; c) Z. Wang, G. Chen, K. Ding, *Chem. Rev.* **2009**, *109*, 322; d) A. Corma, H. Garcia, F. X. L. Xamena, *Chem. Rev.* **2010**, *110*, 4606.
- [10] a) E. Y. Lee, S. Y. Jang, M. P. Suh, *J. Am. Chem. Soc.* **2005**, *127*, 6374; b) P. Leriche, P. Frere, A. Cravino, O. Aleveque, J. Roncali, *J. Org. Chem.* **2007**, *72*, 8332; c) Z.-G. Zhang, K.-L. Zhang, G. Liu, C.-X. Zhu, K.-G. Neoh, E.-T. Kang, *Macromolecules* **2009**, *42*, 3104; d) H. Zhao, W. Z. Yuan, L. Tang, J. Z. Sun, H. Xu, A. Qin, Y. Mao, J. K. Jin, B. Z. Tang, *Macromolecules* **2008**, *41*, 8566.
- [11] a) Z. Li, G. Zhu, X. Guo, X. Zhao, Z. Jin, S. Qiu, *Inorg. Chem.* **2007**, *46*, 5174; b) X. Guo, G. Zhu, F. Sun, Z. Li, X. Zhao, X. Li, H. Wang, S. Qiu, *Inorg. Chem.* **2006**, *45*, 2581; c) B. Zhao, X.-Y. Chen, P. Cheng, D.-Z. Liao, S.-P. Yan, Z.-H. Jiang, *J. Am. Chem. Soc.* **2004**, *126*, 15394; d) B. Chen, L. Wang, F. Zapata, G. Qian, E. B. Lobkovsky, *J. Am. Chem. Soc.* **2008**, *130*, 6718; e) K.-L. Wong, G.-L. Law, Y.-Y. Yang, W.-T. Wong, *Adv. Mater.* **2006**, *18*, 1051.
- [12] a) Y. Xiao, Y. Cui, Q. Zheng, S. Xiang, G. Qian, B. Chen, *Chem. Commun.* **2010**, *46*, 5503; b) B. Chen, L. Wang, Y. Xiao, F. R. Fronczek, M. Xue, Y. Cui, G. Qian, *Angew. Chem. Int. Ed.* **2009**, *48*, 500.
- [13] a) P. Jiang, Z. Guo, *Coord. Chem. Rev.* **2004**, *248*, 205; b) R. Kramer, *Angew. Chem. Int. Ed.* **1998**, *37*, 772; c) L. Fabbri, M. Licchelli, P. Pallavicini, A. Perotti, A. Taglietti, D. Sacchi, *Chem. Eur. J.* **1996**, *2*, 75; d) A. W. Varnes, R. B. Dodson, E. L. Wehry, *J. Am. Chem. Soc.* **1972**, *94*, 946; e) M. Boiocchi, L. Fabbri, M. Licchelli, D. Sacchi, M. Vazquez, C. Zampa, *Chem. Commun.* **2003**, 1812.
- [14] a) X. Zhang, Y. Xiao, X. Qian, *Angew. Chem. Int. Ed.* **2008**, *47*, 8025; b) Z. Xu, K.-H. Baek, H. N. Kim, J. Cui, X. Qian, D. R. Spring, I. Shin, J. Yoon, *J. Am. Chem. Soc.* **2010**, *132*, 601.
- [15] S. Hasegawa, S. Horike, R. Matsuda, S. Furukawa, K. Mochizuki, Y. Kinoshita, S. Kitagawa, *J. Am. Chem. Soc.* **2007**, *129*, 2607.
- [16] a) E. Knoevenagel, *Chem. Ber.* **1894**, *27*, 2345; b) G. Marciniak, A. Delgado, G. Leelere, J. Velly, N. Decken, J. Schwartz, *J. Med. Chem.* **1989**, *32*, 1402; c) L. Rand, J. V. Swisher, C. J. Cronix, *J. Org. Chem.* **1962**, 3505.
- [17] The dimensions given represent maximal cross sections for the molecules, as determined using MOPAC 7.
- [18] a) D. Dang, P. Wu, C. He, Z. Xie, C. Duan, *J. Am. Chem. Soc.* **2010**, *132*, 14321; b) M. North, D. L. Usanov, C. Young, *Chem. Rev.* **2008**, *108*, 5146.
- [19] S. Horike, M. Dinca, K. Tamaki, J. R. Long, *J. Am. Chem. Soc.* **2008**, *130*, 5854.
- [20] O. R. Evans, H. L. Ngo, W. Lin, *J. Am. Chem. Soc.* **2001**, *123*, 10395.
- [21] H. J. Gorvin, *J. Chem. Soc. Perkin Trans. I.* **1988**, 1331.